Published in final edited form as:
Nature. 2010 January 21; 463(7279): 326–330. doi:10.1038/nature08753.

A synchronized quorum of genetic clocks

Tal Danino[1,*], **Octavio Mondragón-Palomino**[1,*], **Lev Tsimring**[2,†], and **Jeff Hasty**[1,2,3,4,†]

[1]Department of Bioengineering, University of California, San Diego, La Jolla, California, USA

[2]BioCircuits Institute, University of California, San Diego, La Jolla, California, USA

[3]Molecular Biology Section, Division of Biological Science, University of California, San Diego, La Jolla, CA 92093, USA

Abstract

The engineering of genetic circuits with predictive functionality in living cells represents a defining focus of the expanding field of synthetic biology. This focus was elegantly set in motion a decade ago with the design and construction of a genetic toggle switch and an oscillator, with subsequent highlights that have included circuits capable of pattern generation, noise shaping, edge detection, and event counting. Here, we describe an engineered gene network with global intercellular coupling that is capable of generating synchronized oscillations in a growing population of cells. Using microfluidic devices tailored for cellular populations at differing length scales, we investigate the collective synchronization properties along with spatiotemporal waves occurring on millimeter scales. We use computational modeling to quantitatively describe the observed dependence of the period and amplitude of the bulk oscillations on the flow rate. The synchronized genetic clock sets the stage for the use of microbes in the creation of a macroscopic biosensor with an oscillatory output. In addition, it provides a specific model system for the generation of a mechanistic description of emergent coordinated behavior at the colony level.

Synchronized clocks are of fundamental importance in the coordination of rhythmic behavior among individual elements in a community or a large complex system. In physics and engineering,the Huygens paradigm of coupled pendulum clocks [1–3] has permeated diverse areas from the development of arrays of lasers [4] and superconducting junctions [5] to GPS [6] and distributed sensor networks [7]. In biology, a vast range of intercellular coupling mechanisms lead to synchronized oscillators which govern fundamental physiological processes such as somitogenesis, cardiac function, respiration, insulin secretion, and circadian rhythms [8–15]. Typically, synchronization helps stabilize a desired behavior arising from a network of intrinsically noisy and unreliable elements. Sometimes, however, the synchronization of oscillations can lead to a severe malfunction of a biological system, as in epileptic seizures [16].

[4]Corresponding Author. Molecular Biology Section, Division of Biological Science, University of California, San Diego, Mailcode 0412, La Jolla, CA 92093-0412, USA. Telephone: 858 822 3442. Fax: 858 534 5722. hasty@ucsd.edu.
[*]These authors contributed equally to this work.
[†]Equal senior investigators.

Supplementary Information
Supplementary information, including methods, supplementary figures and tables, and timelapse microscopy movies, is linked to the online version of the paper at www.nature.com/nature.

Author Information
The authors declare no competing financial interests.

There is considerable interest in the use of synthetic biology to recreate complex cellular behavior from the underlying biochemical reactions that govern gene regulation and signaling. Synthetic biology can be broadly parsed into efforts aimed at the large-scale synthesis of DNA and the forward engineering of genetic circuits from known biological components. In the area of DNA synthesis, pathways have been perturbed and replaced [17] in an effort to understand the network motifs and transcriptional regulatory mechanisms that control cellular processes and elicit phenotypic responses [18]. On a larger scale, progress has been made towards the creation of entire genomes, providing new insights into what constitutes the minimal set of genes required for microbial life [19].

The genetic circuits approach to synthetic biology involves the forward engineering of relatively small gene networks using computational modeling [20, 21]. Here, the original toggle switch [22] and oscillator [23] have inspired the design and construction of circuits capable of controlling cellular population growth [24], generating specific patterns [25], triggering biofilm development [26], shaping intracellular noise [27], detecting edges in an image [28], and counting discrete cellular events [29]. In the context of rhythmic behavior, there have been recent successes in the construction of intracellular oscillators that mimic naturally occurring clocks [30–33]. In addition to their potential as biological sensors, these clock networks have led to insights regarding the functionality of circadian networks [34]. A unifying theme for most of the genetic circuit studies is a particular focus on *dynamical* behavior. Thus the circuits are constructed and monitored in single cells, typically with fluorescent reporters, and new measurement technologies are often developed in parallel [35]. In addition, since nonlinearities and stochasticity arise naturally from the underlying biochemistry, tools from the fields of nonlinear dynamics and statistical physics are extremely useful in both the generation of design specifications and for careful comparison between experiment and computational model.

Synchronized genetic oscillators

The synchronized oscillator design (Fig. 1a) is based on elements of the quorum sensing machineries in *Vibrio fisheri* and *Bacillus Thurigensis*. We placed the *luxI* (from *V. fischeri*), *aiiA* (from *B. Thurigensis*) and *yemGFP* genes under the control of three identical copies of the *luxI* promoter. The LuxI synthase enzymatically produces an acyl-homoserine lactone (AHL), which is a small molecule that can diffuse across the cell membrane and mediates intercellular coupling. It binds intracellularly to the constitutively produced LuxR, and the LuxR-AHL complex is a transcriptional activator for the *luxI* promoter [36]. AiiA negatively regulates the promoter by catalyzing the degradation of AHL[37]. This network architecture, whereby an activator activates its own protease or repressor, is similar to the motif used in other synthetic oscillator designs [30–32] and forms the core regulatory module for many circadian clock networks [13, 38, 39]. In addition, theoretical work has shown how the introduction of an autoinducer in similar designs can potentially lead to synchronized oscillations over a population of cells [40, 41].

Most quorum sensing systems require a critical cell density for generation of coordinated behavior[42]. We modified the local cell density of the synchronized oscillator cells (denoted TDQS1) through the use of microfluidic devices [43] of differing geometries. The device used for monitoring the bulk oscillations consists of a main nutrient-delivery channel that feeds a rectangular trapping chamber (Fig. 1b). Once seeded, a monolayer of *E. coli* cells grow in the chamber and are eventually pushed into the channel where they then flow to the waste port. This device allows for a constant supply of nutrients or inducers and the maintenance of an exponentially growing colony of cells for more than four days. We found that chamber sizes of $100 \times (80–100)\mu m^2$ were ideal for monitoring the intercellular oscillator, as they allowed for sufficient nutrient distribution and optimal cell and AHL densities. In the

context of the design parameters, the flow rate can be modulated in order to change the local concentration of AHL. In addition, the device can be modified in order to permit the observation of spatial waves over longer length scales (see below).

After an initial transient period, the TDQS1 cells exhibit stable synchronized oscillations which are easily discernible at the colony level (Figs. 1c, 1d, and Supplementary Movies 1–2). The dynamics of the oscillations can be understood as follows. Since AHL is swept away by the fluid flow and is degraded by AiiA internally, a small colony of individual cells cannot produce enough inducer to activate expression from the *luxI* promoter. However, once the population reaches a critical density, there is a "burst" of transcription of the *luxI* promoters, resulting in increased levels of LuxI, AiiA, and GFP. As AiiA accumulates, it begins to degrade AHL, and after a sufficient time, the promoters return to their inactivated state. The production of AiiA is then attenuated, which permits another round of AHL accumulation and another burst of the promoters.

In order to determine how the effective AHL dissipation rate affects the period of the oscillations, we conducted a series of experiments at various channel flow rates. At high flow rate, the oscillations stabilize after an initial transient and exhibit a mean period of 90±6 minutes and mean amplitude of 54±6 GFP AU (Fig. 2a, Supplementary Movie 2). At low flow rate, we observed a period of 55±6 minutes and an amplitude of 30±9 GFP AU. Interestingly, the waveforms have differing shape, with the slower oscillator reaching a trough near zero after activation and the faster oscillator decaying to levels above the original baseline (Fig. 2b). We swept the flow rate from 180 to 296 μm/min and observed an increasing oscillatory period from 52–90 minutes (Fig. 2c). In addition, we found the amplitude to be proportional to the period of the oscillations (Fig. 2d), which is consistent with "degrade-and-fire" oscillations [44] observed in a previously reported intracellular oscillator [31].

In experiments conducted at low flow rate, we observed the spatial propagation of the fluorescence signal across the 100 μm chamber. In order to investigate these spatiotemporal dynamics in more detail, we redesigned the microfluidic chip with an extended 2 mm trapping chamber (Supplementary Information). Snapshots of a typical experimental run are presented in Fig. 3a (Supplementary Movies 3 and 4). A few isolated colonies begin to grow and subsequently merge into a large monolayer that fills the chamber (Fig. 3a: 66 minutes). At 100 minutes, there is a localized burst of fluorescence that propagates to the left and right in subsequent frames (Fig. 3a: 100–118 minutes). A second burst occurs near the original location and begins to propagate to the left and right as before.

Spatiotemporal Dynamics

To illustrate the spatiotemporal information contained in an entire 460-minute image sequence, we plot the fluorescence intensity as a function of time and distance along the chamber (Fig. 3b). Note the correspondence of this space-time plot to the images in Fig. 3a. During the first 100 minutes, there is no activity and the space-time plot is blue, indicating no fluorescence. Then at 100 minutes, there is an orange spot at around 1350 μm, corresponding to the burst in Fig. 3a. In the space-time plot, propagation of a wave to the left and right appears as an green-yellow concave line. The larger slope to the left of the burst-origin indicates that the leftward moving wave is traveling slower (~25μm/min) than the rightward wave (~35μm/min). Subsequent waves originating from a nearby location arise as additional orange-yellow intensity lines. These intensity lines indicate "annihilation events", where a leftward moving and rightward moving waves collide and annihilate each other. While these events are striking in the movies (Supplementary Movies 3 and 4), they appear subtly in the space-time plot at locations where positive and negative slopes meet

(300–400 μm in 2nd intensity line and on). As the traveling wave gets further from a burst location it breaks off into a packet (170 minutes) which travels leftward at 12.5 μm/min initially, and slows to 8.5 μm/min towards the end of the trap where the cell density is lower (between 118–200 minutes). The corresponding cell-density space-time plot shows that a higher density of cells is first reached at the center of the colony and is minimal towards the left-moving edge (Fig. 3c and Supplementary Movie 3). As a result, the critical cell and AHL densities for wave propagation are reached at different times and spatial locations.

We also investigated how the intercellular oscillator behaves in a three-dimensional colony growing in a 400×1000×4.0 μm^3 microfluidic chamber (Figs. 3d, 3e, and Supplementary Movie 5). In this device, the colony grows radially over the course of 180 minutes without fluorescing until it reaches a size of approximately 100 μm. At this time, a large fluorescence burst originates from the center of the colony, with a bright band near the center (Fig. 3d: 228 minutes). During this first burst (273 minutes), the bright band shows that cells at an intermediate cell density have a larger amplitude and longer period than cells near the front or in the interior. As the colony expands an additional 50–100 μm in diameter, a second burst of fluorescence occurs at a similar intermediate cell density. Subsequent oscillations are seen as the cell growth front propagates, while weak oscillations arise and quickly die inside the colony.

Quantitative modeling

In order to quantitatively describe the mechanisms driving bulk synchronization and wave propagation, we developed a computational model using delayed differential equations for protein and AHL concentrations (Supplementary Information). While conceptually the nature of oscillations is reminiscent of the degrade-and-fire oscillations observed in a dual delayed feedback circuit [31, 44], an important difference is the coupling among genetic clocks in different cells through extracellular AHL. The modeling of this coupling, and the related cell density dependence, allowed us to explain most of the non-trivial phenomenology of the spatiotemporal quorum clock dynamics.

A broad range of model parameters lead to oscillations (Figs. 4a–d), though there is a distinct absence of oscillations at small and large cell densities for low to medium flow values (Fig. 4c). The qualitative nature of the oscillations can be explained using Fig. 4a. Each period begins with the latent accumulation of both AiiA and LuxI, which after a delay burst rapidly to high values. That burst suppresses AHL and further production of AiiA and LuxI. Both of these proteins then decay enzymatically, after which the process repeats. As expected, the period of the oscillations is roughly proportional to the enzymatic protein decay time. The period grows with the external AHL flow rate (effective degradation) and the amplitude of the oscillations, in good agreement with the experiments (compare Fig. 4b with Figs. 3c and d).

We modeled the collective spatiotemporal dynamics of the clocks by generalizing the bulk model to include the coupling of individual oscillators through extracellular AHL. The model consists of a one-dimensional array of “cells”, each of which is described by the same set of delay-differential equations coupled to a common, spatially nonuniform field of extracellular AHL. The latter is described by a linear diffusion equation with sources and sinks due to AHL diffusion through the cell membrane and dilution. A small AHL perturbation in the middle of the array initiates waves of LuxI concentration (Fig. 4c), in excellent agreement with the experimental findings (compare Figs. 3b and 4c). The velocity of the front propagation depends on the external AHL diffusion coefficient D_1 (Fig. 4d and Supplementary Information), and for experimentally relevant values of D_1, the simulated front velocity is in good agreement with experimental data. In addition, cell density plays an

important role in wave propagation. In order to model the evolution of the three-dimensional colony (Figs. 3c and 3d), we set the functional form of the cell density to be an expanding "Mexican hat", as observed in the experiments. Oscillations are then suppressed by the high density of cells in the middle of the colony, and LuxI bursts only occur on the periphery of the growing colony of cells. This phenomenology is also in excellent agreement with our experimental findings (compare Figs. 4f and 3d).

Emergence

On a fundamental level, the synchronized oscillations represent an emergent property of the colony that can be mechanistically explained in terms of the circuit design. Oscillations arise because the small molecule AHL plays a dual role, both enabling activation of the genes necessary for intracellular oscillations and mediating the coupling between cells. Since unbounded growth of the colony leads to an accumulation of AHL that ultimately quenches the bulk oscillations, we used open-flow microfluidic devices to allow for the flow of AHL away from the colony. At low cell densities, oscillations do not occur because intracellular gene activation is decreased as AHL diffuses across the cell membrane and out of the chamber. At intermediate cell densities (i.e. a full chamber), the increased production of AHL in each cell acts to mitigate the outward flow such that activation of the genes can occur in a rhythmic fashion, and colony-wide oscillations emerge in a seemingly spontaneous fashion.

A natural question arises regarding the behavior of individual cells in the absence of coupling. While experimentally we cannot turn off the coupling while maintaining intracellular gene activation, we addressed this question using simulations by artificially setting the AHL diffusion rate across the cell membrane to zero (with the other parameters fixed). We find that individual cells oscillate independently for any cell density since they are completely decoupled from the environment and each other. This result indicates that the coupling through AHL diffusion provides a means for the synchronization of individual oscillators at intermediate cellular concentrations.

Perspective and outlook

In the mid seventeenth century, Chirstiaan Huygens serendipitously observed that two pendulum clocks oscillated in synchrony when mounted to a common support beam [1]. While observations of synchronization in nature surely predate the age of enlightenment, Huygens is credited as the first to systematically characterize the synchronization of oscillators in terms of a known coupling mechanism (which, in the case of the pendula, he deduced as vibrations in the common support). We have shown how quorum sensing can be used to couple genetic clocks, leading to synchronized oscillations at the colony level. Given the single-cell variability and intrinsic stochasticity of most synthetic gene networks [27, 30, 31, 45, 46], the use of quorum sensing is a promising approach to increasing the sensitivity and robustness of the dynamic response to external signals. Along these lines, our results set the stage for the design of networks that can function as spatially distributed sensors or synthetic machinery for coupling complex dynamical processes across a multicellular population.

Methods

Strains, growth conditions

Three identical transcriptional cassettes for *luxI, aiiA*, and *yemGFP* were constructed by replacing a modular pZ plasmid's promoter [47] (with *yemGFP*) with the lux operon from the native *Vibrio Fischeri* operon (*luxR* up to *luxI* stop codon) [48]. *LuxI* and *aiiA* [49] genes were

cloned in place of *yemGFP* and a degradation tag was added to the carboxy-terminal of each. A previously used MG1655 strain of Escherichia coli[1] was transformed with plasmids pTD103luxI/GFP(colE1,Kan) and pTD103aiiA(p15A,Amp) to create strain TDQS1 (Suppl. Info).

Each experiment started with a 1:1000 dilution of overnight culture grown in 50mL LB (10g/L NaCl) with antibiotics 100μg/ml ampicillin(Amp) and 50μg/ml kanamycin(Kan) for approximately 2 hours. Cells reached an OD600 of 0.05–0.1 and were spun down and concentrated in 5mL of fresh media with surfactant concentration of 0.075 Tween20 [Sigma-Aldrich, St.Louis,MO] before loading in a device.

Microfluidics and Microscopy

Images were acquired using an epifluorescent inverted microscope (TE2000-U, Nikon Instruments Inc., Tokyo, Japan), and chip temperatures were maintained at 37°C with a plexiglass incubation chamber encompassing the entire microscope. Phase contrast and fluorescent images were taken at 20× or 60× every 2–5 minutes and focus was maintained automatically using Nikon Elements software.

Supplementary Material

Refer to Web version on PubMed Central for supplementary material.

Acknowledgments

We thank Jesse Stricker for helpful discussions on plasmid construction, and Matt Bennett, Kurt Wiesenfeld, and Jim Collins for stimulating discussions during the preparation of the manuscript. This work was supported by the National Institutes of Health and General Medicine (GM69811), the DOE CSGF fellowship (TD), and CONACyT (Mexico, grant 184646, OMP).

References

1. Huygens, C. Œuvres complètes de Christiaan Huygens. Vol. vol. 17. The Hague: Martinus Nijhoff; 1932.
2. Pikovsky, A.; Rosenblum, M.; Kurths, J. Synchronization: A Universal Concept in Nonlinear Sciences. Cambridge, England: 2001.
3. Strogatz, S. Sync. New York: Penguin Books; 2004.
4. Vladimirov A, Kozyreff G, Mandel P. Synchronization of weakly stable oscillators and semiconductor laser arrays. Europhysics Letters 2003;61:613–619.
5. Wiesenfeld K, Colet P, Strogatz S. Synchronization transitions in a disordered Josephson series array. Physical Review Letters 1996;76:404–407. [PubMed: 10061448]
6. Lewandowski W, Azoubib J, Klepczynski W. GPS: primary tool for time transfer. Proceedings of the IEEE 1999;87:163–172.
7. Li D, Wong K, Hu Y, Sayeed A. Detection, classification and tracking of targets in distributed sensor networks. IEEE Signal Processing Magazine 2002;19:17–29.
8. Winfree A. Biological rhythms and the behavior of populations of coupled oscillators. Journal of Theoretical Biology 1967;16:15. [PubMed: 6035757]
9. Mirollo R, Strogatz S. Synchronization of pulse-coupled biological oscillators. SIAM Journal on Applied Mathematics 1990:1645–1662.
10. Elson R, et al. Synchronous behavior of two coupled biological neurons. Physical Review Letters 1998;81:5692–5695.
11. Jiang Y, et al. Notch signalling and the synchronization of the somite segmentation clock. Nature 2000;408:475–478. [PubMed: 11100729]
12. Glass L. Synchronization and rhythmic processes in physiology. Nature 2001;410:277–284. [PubMed: 11258383]

13. Young M, Kay S. Time zones: a comparative genetics of circadian clocks. Nature Reviews Genetics 2001;2:702–715.
14. Chabot J, Pedraza J, Luitel P, van Oudenaarden A. A. Stochastic gene expression out-of-steady-state in the cyanobacterial circadian clock. Nature 2007;450:1249–1252. [PubMed: 18097413]
15. Kerckhoffs R, McCulloch A, Omens J, Mulligan L. Effects of biventricular pacing and scar size in a computational model of the failing heart with left bundle branch block. Medical Image Analysis 2009;13:362–369. [PubMed: 18675578]
16. Grenier F, Timofeev I, Steriade M. Neocortical very fast oscillations (ripples, 80–200 Hz) during seizures: intracellular correlates. Journal of Neurophysiology 2003;89:841. [PubMed: 12574462]
17. Isalan M, et al. Evolvability and hierarchy in rewired bacterial gene networks. Nature 2008;452:840. [PubMed: 18421347]
18. Alon U. Network motifs: theory and experimental approaches. Nature Reviews Genetics 2007;8:450–461.
19. Gibson D, et al. Complete chemical synthesis, assembly, and cloning of a Mycoplasma genitalium genome. Science 2008;319:1215. [PubMed: 18218864]
20. Hasty J, McMillen D, Collins J. Engineered gene circuits. Nature 2002;420:224–230. [PubMed: 12432407]
21. Endy D. Foundations for engineering biology. Nature 2005;438:449–453. [PubMed: 16306983]
22. Gardner T, Cantor C, Collins J. Construction of a genetic toggle switch in Escherichia coli. Nature 2000;403:339–342. [PubMed: 10659857]
23. Elowitz MB, Leibler S. A synthetic oscillatory network of transcriptional regulators. Nature 2000;403:335–338. [PubMed: 10659856]
24. You L, Cox R, Weiss R, Arnold F. Programmed population control by cell-cell communication and regulated killing. Nature 2004;428:868–871. [PubMed: 15064770]
25. Basu S, Gerchman Y, Collins C, Arnold F, Weiss R. A synthetic multicellular system for programmed pattern formation. Nature 2005;434:1130–1134. [PubMed: 15858574]
26. Kobayashi H, et al. Programmable cells: interfacing natural and engineered gene networks. Proceedings of the National Academy of Sciences 2004;101:8414–8419.
27. Austin D, et al. Gene network shaping of inherent noise spectra. Nature 2006;439:608–611. [PubMed: 16452980]
28. Tabor J, et al. A Synthetic Genetic Edge Detection Program. Cell 2009;137:1272–1281. [PubMed: 19563759]
29. Friedland A, et al. Synthetic Gene Networks That Count. Science 2009;324:1199. [PubMed: 19478183]
30. Atkinson M, Savageau M, Myers J, Ninfa A. Development of genetic circuitry exhibiting toggle switch or oscillatory behavior in Escherichia coli. Cell 2003;113:597–607. [PubMed: 12787501]
31. Stricker J, et al. A fast, robust and tunable synthetic gene oscillator. Nature 2008;456:516–519. [PubMed: 18971928]
32. Tigges M, Marquez-Lago T, Stelling J, Fussenegger M. A tunable synthetic mammalian oscillator. Nature 2009;457:309–312. [PubMed: 19148099]
33. Fung E, et al. A synthetic gene-metabolic oscillator. Nature 2005;435:118–122. [PubMed: 15875027]
34. Cookson NA, Tsimring LS, Hasty J. The pedestrian watchmaker: Genetic clocks from engineered oscillations. FEBS Letters. 2009
35. Bennett MR, Hasty J. Microfluidic devices for measuring gene network dynamics in single cells. Nature Reviews Genetics 2009;10:628–638.
36. Waters C, Bassler B. Quorum sensing: cell-to-cell communication in bacteria. Annual Review of Cell and Developmental Biology. 2005
37. Liu D, et al. Mechanism of the Quorum-Quenching Lactonase (AiiA) from Bacillus thuringiensis. 1. Product-Bound Structures. Biochemistry 2008;47:7706–7714. [PubMed: 18627129]
38. Glossop N, Lyons L, Hardin P. Interlocked feedback loops within the Drosophila circadian oscillator. Science 1999;286:766. [PubMed: 10531060]

39. Lakin-Thomas P, Brody S. Circadian rhythms in microorganisms: new complexities. Annu. Rev. Microbiol. 2004
40. McMillen D, Kopell N, Hasty J, Collins J. Synchronizing genetic relaxation oscillators by intercell signaling. Proceedings of the National Academy of Sciences 2002;99:679–684.
41. Garcia-Ojalvo J, Elowitz M, Strogatz S. Modeling a synthetic multicellular clock: Repressilators coupled by quorum sensing. Proceedings of the National Academy of Sciences 2004;101:10955–10960.
42. Reading N, Sperandio V. Quorum sensing: the many languages of bacteria. FEMS Microbiology Letters 2006;254:1–11. [PubMed: 16451172]
43. Cookson S, Ostroff N, Pang W, Volfson D, Hasty J. Monitoring dynamics of single-cell gene expression over multiple cell cycles. Molecular Systems Biology 2005;1
44. Mather W, Bennett M, Hasty J, Tsimring L. Delay-induced degrade-and-fire oscillations in small genetic circuits. Physical Review Letters 2009;102:68105.
45. Ozbudak E, Thattai M, Kurtser I, Grossman A, van Oudenaarden A. Regulation of noise in the expression of a single gene. Nature Genetics 2002;31:69–73. [PubMed: 11967532]
46. Elowitz M, Levine A, Siggia E, Swain P. Stochastic gene expression in a single cell. Science 2002;297:1183. [PubMed: 12183631]
47. Lutz R, Bujard H. Independent and tight regulation of transcriptional units in Escherichia coli via the LacR/O, the TetR/O and AraC/I1-I2 regulatory elements. Nucleic Acids Research 1997;25:1203. [PubMed: 9092630]
48. Dunlap P, Greenberg E. Control of Vibrio fischeri luminescence gene expression in Escherichia coli by cyclic AMP and cyclic AMP receptor protein. Journal of Bacteriology 1985;164:45–50. [PubMed: 2995319]
49. Thomas P, et al. The quorum-quenching lactonase from Bacillus thuringiensis is a metallo-protein. Biochemistry(Washington) 2005;44:7559–7569.

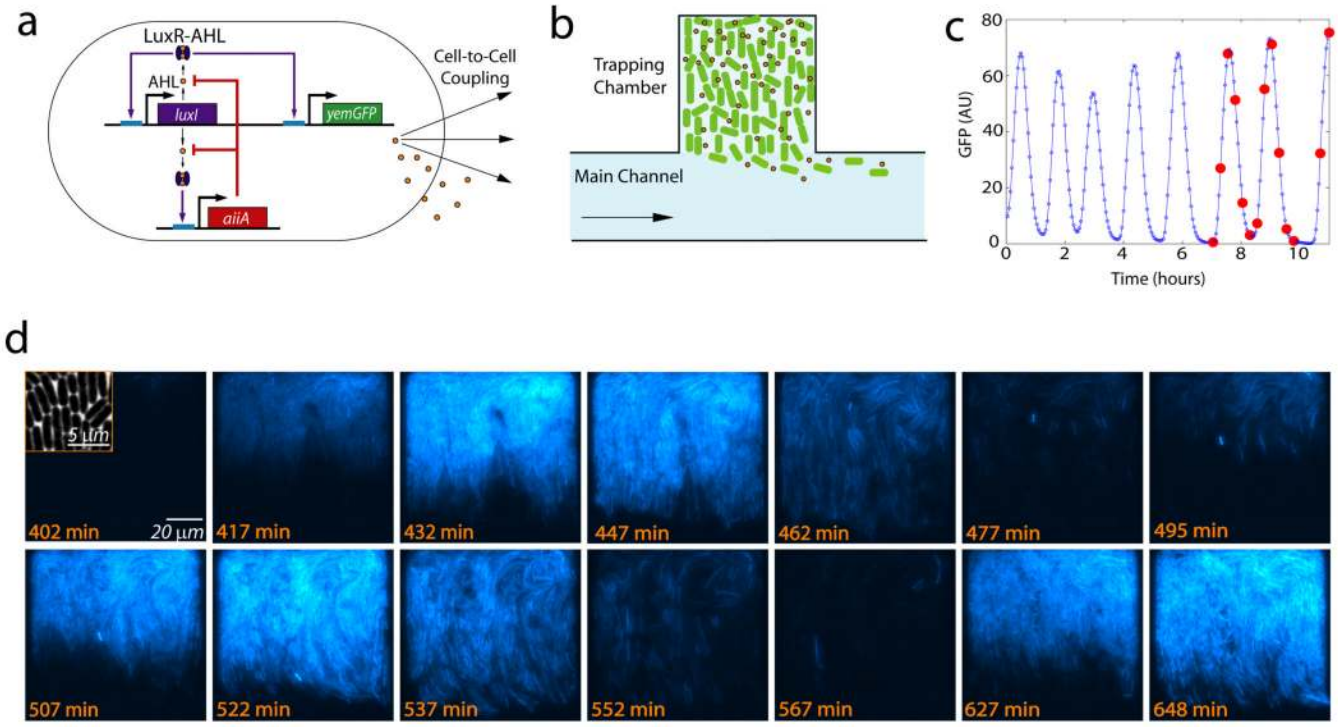

Figure 1.

Synchronized genetic clocks. (**a**) Network Diagram. The *luxI* promoter drives production of the *luxI, aiiA*, and *yemGFP* genes in three identical transcriptional modules. LuxI enzymatically produces a small molecule AHL, which can diffuse outside of the cell membrane and into neighboring cells, activating the *luxI* promoter. AiiA negatively regulates the circuit by acting as an effective protease for AHL. (**b**) Microfluidic device used for maintaining *E. coli* at a constant density. The main channel supplies media to cells in the trapping chamber, and the flow rate can be externally controlled in order to change the effective degradation rate of AHL. (**c**) Bulk fluorescence as a function of time for a typical experiment in the microfludic device. The red circles correspond to the image slices in (**d**). (**d**) Fluorescence slices of a typical experimental run demonstrate synchronization of oscillations in a population of *E.coli* residing in the microfluidic device (Supplementary Movie 1). Inset in the first snapshot is a 100× zoom of cells.

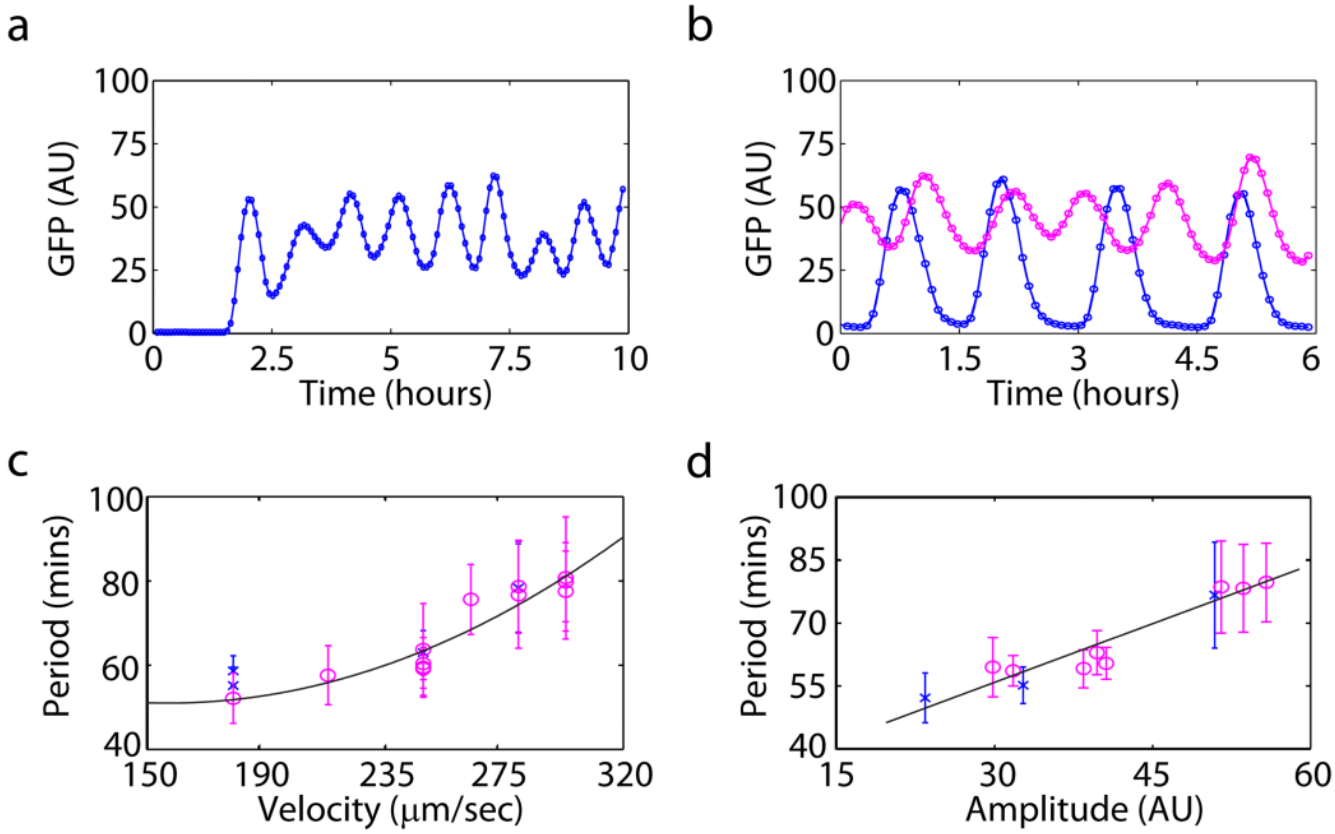

Figure 2.
Dynamics of the synchronized oscillator under multiple microfluidic flow conditions (Supplementary Movies 1 and 2). (**a**) At around 90 minutes, cells begin to oscillate synchronously after reaching a critical density in the trap. (**b**) The period and amplitude increase for higher flow rates. Magenta curve is at low velocity(240μm/min), blue is at higher velocity(280μm/min). (**c**) Period as a function of velocity in the main channel showing tunability of period between 55–90 minutes. (**d**) Period vs. amplitude for all experiments. Magenta circles (**c,d**) are data from 84 and 90μm traps, blue crosses are 100μm traps.

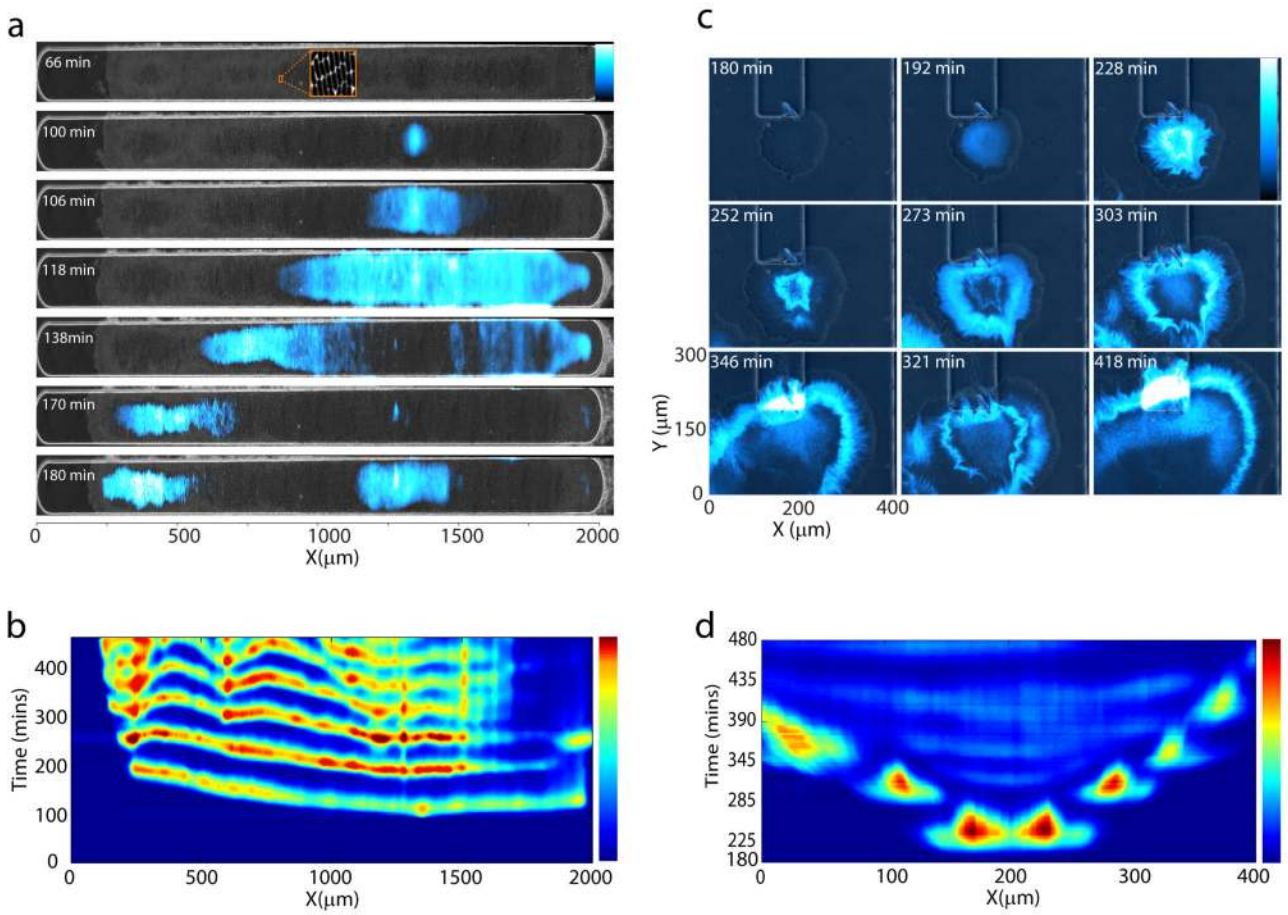

Figure 3.

Spatiotemporal dynamics of the synchronized oscillators. (**a**) Snapshots of the GFP fluorescence superimposed over brightfield images of a densely packed monolayer of *E. coli* cells are shown at different times after loading (Supplementary Movies 3 and 4). Traveling waves emerge spontaneously in the middle of the colony and propagate outwards with the speed of ~8-35μm/min. At later times waves partially lose coherence due to inhomogeneity in cell population and intrinsic instability of wave propagation (see Modeling Box). (**b**) Corresponding space-time diagram showing the fluorescence of cells along the center of the trap as a function of time. (**c**) Snapshots of the GFP fluorescence superimposed over the brightfield images of a three-dimensional growing colony of *E. coli* cells at different times after loading (Supplementary Movie 5). Bursts of fluorescence begin when the growing colony reaches a critical size of about 100μm. These bursts are primarily localized at the periphery of the growing colony. (**d**) Corresponding space-time diagram showing fluorescence of cells along a horizontal line through the center of the growing colony.

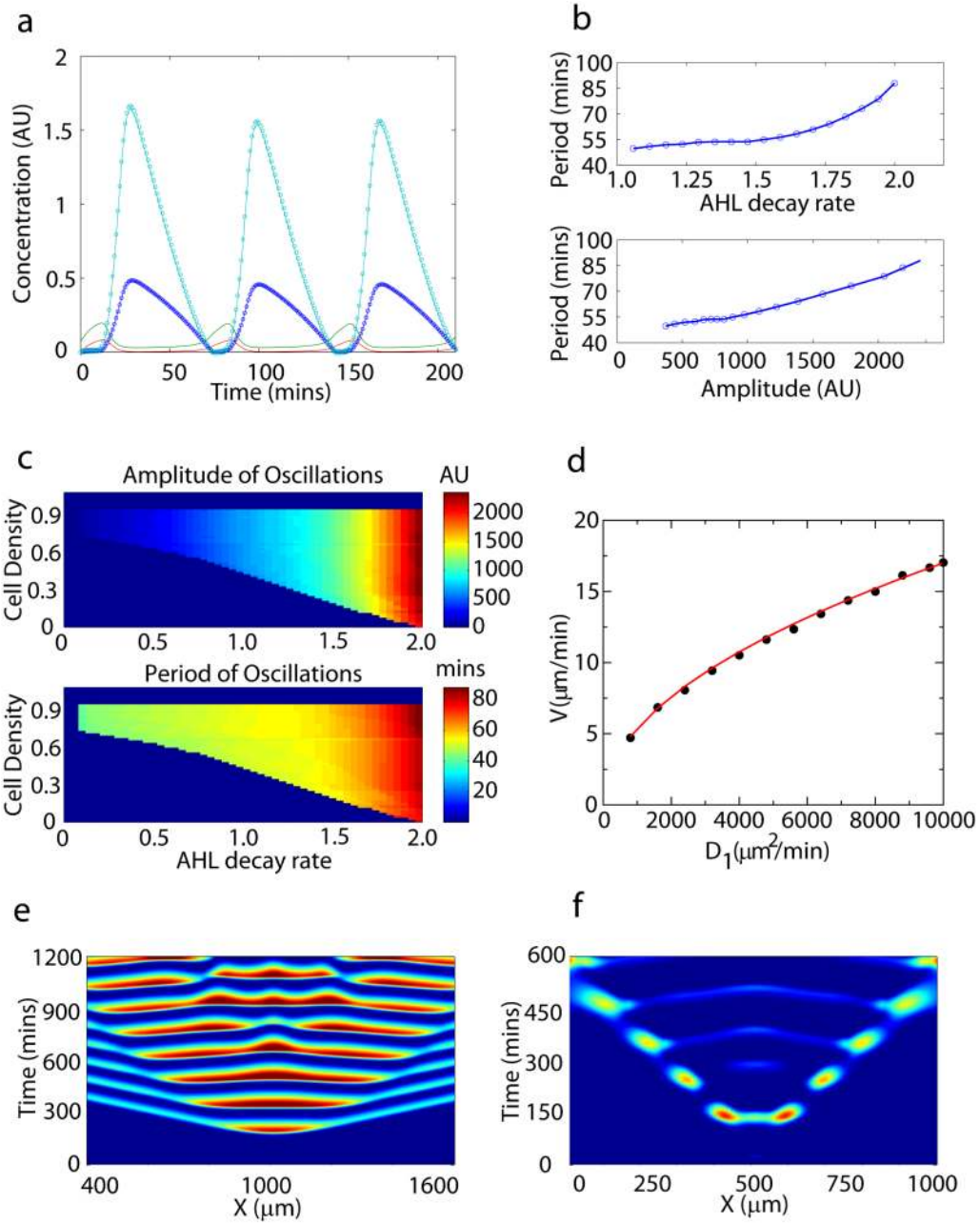

Figure 4.

Modeling of synchronized genetic clocks. (**a**) A typical time series of concentrations of LuxI (cyan circles), AiiA (blue circles), internal AHL (green line), and external AHL (red line). LuxI and AiiA closely track each other, and are anti-phase with the concentrations of external and internal AHL. (**b**) Period of oscillations as a function of the flow rate μ at cell density $d = 0.5$ (top panel). Period as a function of the amplitude of oscillations for the same cell density (bottom panel). (**c**) Period and amplitude as a function of cell density and AHL decay rate μ. Oscillations occur over a finite range of cell densities, and period increases with μ after the bifurcation line is crossed. The results in (**c**) and (**d**) compare favorably with the experimental results in Figs. 2c and 2d. (**d**) Speed of wave front propagation as a function of the diffusion coefficient D_1. The numerical data scale as $V \sim D_1^{1/2}$ (red line). (**e**)

Space-time diagram of traveling waves propagating through a uniform array of cells corresponding to the experiment depicted in Figs. 3a and 3b. (**f**) Space-time diagram of bursting oscillations in a growing0020cell population corresponding to the experiments in Figs. 3c and 3d.